International Journal of Civil Engineering (2022) 20:195–206
https://doi.org/10.1007/s40999-021-00679-9

RESEARCH PAPER

Centrifuge Modelling of Monopiles in Calcareous Sand Subjected to Cyclic Lateral Loading

Roozbeh Rezanejad Malakshah[1] · Majid Moradi[1] · Abbas Ghalandarzadeh[1]

Received: 27 February 2021 / Revised: 13 July 2021 / Accepted: 15 September 2021 / Published online: 22 October 2021

Abstract
Monopiles are the most common foundation type for offshore wind turbines. These structures are subjected to millions of cyclic horizontal loads during their lifespans, mainly from waves and wind; however, there are gaps in conventional design methods for different aspects of cyclic loading. The present study examined the cyclic behaviour of monopiles in dry calcareous sand. Centrifuge tests were carried out to investigate the effect of cyclic loading on the accumulated displacement and soil-pile stiffness. The results showed that asymmetric two-way loading is the most damaging load type, although its difference from one-way loading is less than what has been reported previously. Asymmetric two-way loading was found to cause up to 20% more displacement than one-way loading. Furthermore, the secant stiffness of the soil-pile system increased about 15% after 600 cycles, and a logarithmic function has been provided to describe this trend. The slope of this function increased with the maximum cyclic load magnitude; however, an increase in the cyclic load magnitude decreased the soil-pile stiffness. Moreover, the soil-pile stiffness was considerably lower in symmetric two-way loading compared to other load reversal conditions. After each cyclic test, monotonic loading was applied. In most cases, the post-cyclic lateral capacity was nearly equal to the static capacity. A model is proposed to predict the accumulated displacement under cyclic loading.

Keywords Monopiles · Offshore wind turbines · Calcareous sands · Centrifuge modelling

1 Introduction

Offshore wind turbines (OWTs) have developed rapidly as an alternative to fossil fuel as an energy source. Monopiles are both cost-effective and easy to implement; thus, they are the most common foundations for offshore wind turbines. Monopiles are large-diameter piles with an embedment length-to-diameter ratio (L/D) of less than 10 [1]. OWTs tolerate different load combinations, including both horizontal and vertical loads. Horizontal loads resulting from wave action and wind are the primary cause of concern when designing OWT foundations.

The conventional p–y method used by API [2] and DNV [3] is based on the results of experiments conducted with slender piles having a diameter of less than 1 m and with a small load eccentricity [4, 5]. This means that the reliability of this method for the design of large-diameter piles is in question [6–8]. Furthermore, these guidelines have been developed for the offshore oil and gas sector, from which the loading characteristics of OWTs differ.

An OWT is subjected to millions of cycles during its lifespan. This cyclic loading could cause accumulated rotation of the structure. Current guidelines use a simple approach for considering the effect of cyclic loading. API [2] considers a different calibration factor for lateral resistance in the case of cyclic loading. This factor is independent of the number of load cycles, load magnitude and symmetry. An accurate prediction of accumulated rotation and changes in stiffness caused by cyclic loading is vital when designing monopile foundations. For this

✉ Majid Moradi
mmoradi@ut.ac.ir

Roozbeh Rezanejad Malakshah
rezanejad.r@ut.ac.ir

Abbas Ghalandarzadeh
aghaland@ut.ac.ir

1 School of Civil Engineering, College of Engineering, University of Tehran, Tehran, Iran

reason, many researchers have begun to study the cyclic behaviour of piles, particularly monopiles [9–16].

Little and Briaud [17] introduced a power function based on pressuremeter tests as a degradation factor for soil resistance. This function considers the effect of the number of cycles. Other studies have proposed degradation functions which considered parameters such as the soil density, installation method and cyclic loading ratio [18, 19]. These studies have been done on long flexible piles, and the number of load cycles was limited. Their results suggested that one-way loading caused greater displacement than two-way loading; however, recent studies have reported that asymmetric two-way loading generated more displacement than one-way loading [10, 11, 20, 21].

LeBlanc et al. [20] studied the effect of long-term cyclic loading on stiff piles in dry, loose sand using small-scale laboratory modelling. Their results indicated that the power function was the best fit for the accumulated rotation of piles under cyclic lateral loading. They introduced ζ_b and ζ_c to describe the loading characteristics as follows:

$$\zeta_{\mathrm{b}} = \frac{M_{\max}}{M_{\mathrm{r}}} = \frac{F_{\max}}{F_{\mathrm{r}}}, \tag{1}$$

$$\zeta_{\mathrm{c}} = \frac{M_{\min}}{M_{\max}} = \frac{F_{\min}}{F_{\max}}, \tag{2}$$

where $M_{\min}$ and $M_{\max}$ are the minimum and maximum moments at the mudline, respectively, and M_{r} is the moment at failure or at a specific rotation at the mudline. They proposed the following equation for accumulated rotation:

$$\frac{\Delta\theta(N)}{\theta_{\mathrm{s}}} = T_{\mathrm{b}}(\zeta_{\mathrm{b}}.R_{\mathrm{d}})T_{\mathrm{c}}(\zeta_{\mathrm{c}}).N^{\alpha}, \tag{3}$$

where N is the number of cycles, R_{d} is the relative density of the soil, θ_{s} is the rotation under static loading, $\Delta\theta_N$ is the increase in rotation after N cycles, α is an accumulation parameter and T_{b} and T_{c} are dimensionless functions that depend on the loading characteristics and relative density.

Their results showed that the largest number of rotations occurred at $\zeta_c = -0.6$, which indicates asymmetric two-way loading. Klinkvort and Hededal [22] used a similar model for predicting the accumulated rotations. They investigated the behaviour of monopiles in saturated and dry sand using centrifuge tests. In contrast to the previous research, their results showed that one-way loading was the most damaging load condition. Furthermore, they noted that the foundation stiffness increased with an increase in N, as has been documented by Refs. [20, 23]. This contradicts the findings of Achmus et al. [13], API [2] and DNV [3]. The primary cause for this contradiction could be that each researcher used a different definition of foundation stiffness [24, 25].

Albiker et al. [26] carried out a series of 1 g model tests on rigid and flexible piles. Their results indicated that, in the case of rigid piles, asymmetric two-way loading caused the maximum displacement accumulation, and the loading function (T_{c}) was not affected by system parameters such as the pile stiffness and relative density of the sand. In the case of flexible piles, one-way loading was the most damaging load condition.

Nicolai et al. [14] investigated the effect of cyclic loading on the post-cyclic capacity of monopiles in dense silica sand. In both the centrifuge and 1 g tests, the post-cyclic capacity increased with the magnitude of the cyclic load and the number of loading cycles. This increase was more significant when the loading symmetry approached balanced two-way loading. On the other hand, centrifuge tests conducted by Truong et al. [27] indicated that the post-cyclic capacity was equal to or less than the static capacity.

The results of various studies show inconsistency related to issues such as soil-pile stiffness, displacement prediction functions, the effect of load symmetry on displacement and the post-cyclic capacity. All studies discussed above were carried out on siliceous sand, although about 40% of the ocean floor is covered by calcareous sediment [28]. These biogenic materials, formed mainly from shell fragments and coral reef detritus, are commonly found at low latitudes in tropical areas such as the Persian Gulf.

Because of its high particle angularity, high void ratio and particle crushability, the engineering properties of calcareous sand differ from those of siliceous sand [29]. The pile capacity in calcareous sediment has been a focus of study in geotechnical engineering. Most studies have concentrated on the axial capacity of the piles, but a few researchers have addressed the problem of monotonic lateral loading of piles in calcareous sand [30, 31]. These studies suggest that the existing method underestimates pile resistance in the case of large displacement in calcareous sand; however, no studies were found that investigated the cyclic lateral behaviour of monopiles in this type of sand.

The present study explored the cyclic behaviour of monopiles in calcareous sand by means of centrifuge modelling. The effect of cyclic loading and its characteristics on the accumulated deformation and soil-pile stiffness have been compared with the findings of previous works. The effect of cyclic loading on the ultimate resistance of the monopiles also has been investigated, and a model is proposed to predict the accumulated displacement of the pile head based on the method introduced by LeBlanc et al. [20].

2 Experimental Procedure

All testing were carried out using the geotechnical centrifuge provided by the University of Tehran. The rotation radius and maximum acceleration of the beam centrifuge were 3 m and 130 g, respectively. More details about this apparatus can be found in Moradi et al. [32]. All centrifuge tests were conducted at a gravity level of 40 g, which translates to a scaling factor of 40. A servo-motor was used to generate the cyclic loads, which were applied at 5.75*D* (*D* = diameter of the monopile) above the mudline. The rotary motion was converted to linear motion using a ball-screw mechanism. To allow free rotation at the loading point, a hinge connection between the monopile and transition piece was designed that is similar to the one employed by Choo and Kim [33]. A sketch and a photo of the setup are shown in Figs. 1 and 2, respectively.

The model monopile had a stainless-steel tubular profile that was 50.8 mm in diameter and 1 mm in thickness. The pile diameter (*D*), after coating, was 52 mm (208 cm at prototype scale). It had an embedment length of 5*D* and was instrumented with ten pairs of strain gauges (TML-FLA-5-11; Tokyo Sokki Kenkyujo). Each pair of gauges was arranged in a half-bridge Wheatstone configuration to measure the bending moment. The first pair was installed at 10 mm above the pile tip and the centre-to-centre spacings were 30 mm.

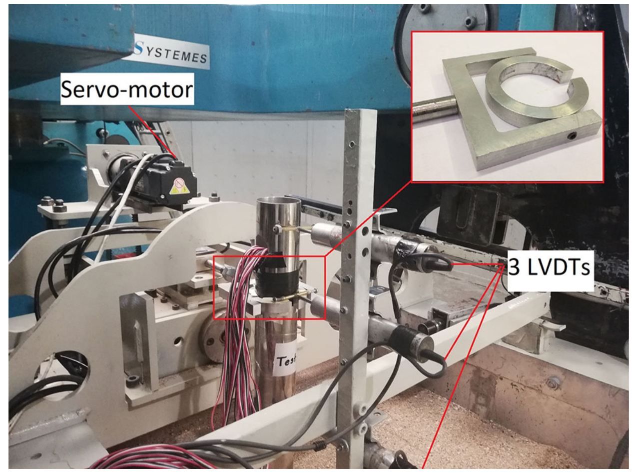

Fig. 2 Centrifuge model setup

Poulos and Hull [34] introduced pile-soil relative stiffness ($E_P I_P / E_s L^4$) to consider the effect of pile rigidity on the pile response where E_s and E_p are the elastic modulus

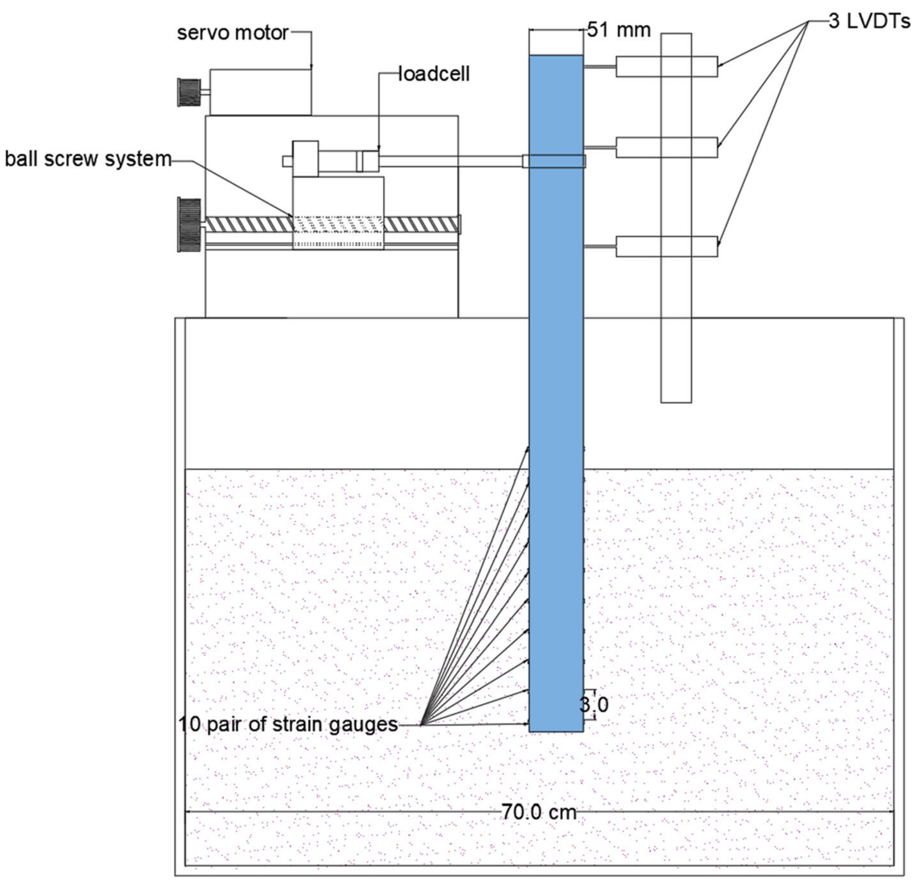

Fig. 1 Sketch of the test setup

of the soil and pile, respectively, I_p is the moment of inertia of the pile and L is the embedment length. By considering E_s = 50 MPa, based on estimates of Abadie [35], the ratio for the monopile in the present study would be approximately 0.04, which is similar to some monopiles used in industry [35].

The lateral displacement of the pile shaft was measured by three linearly variable differential transformers (LVDTs) at levels of 16 cm, 30 cm and 38 cm above the mudline (model scale). Two of them were positioned above the loading point to allow calculation of the rotation of the monopile head. After obtaining the deflection and rotation of one point as well as the bending moment diagram, displacement along the monopile length could be calculated using classic beam theory, as shown in Eq. (4). In this research, classic beam theory was only used to calculate the pile deflection and rotation at the mudline. It should be noted that the bending moment diagram along the free length of the monopile was linear:

$$E_P I_P \frac{d_y^2}{d_x^2} = M(x). \tag{4}$$

All samples were prepared in a strongbox with a width of 60 cm, a length of 70 cm and a height of 55 cm. The box length was greater than 10*D*, which was sufficient to allow the boundary effect to be disregarded, as demonstrated in previous studies [36–38]. Calcareous sand from Hormuz Island in the northern Persian Gulf was used for the experiments. All tests were carried out in dense sand because monopiles are usually placed under similar conditions [1]. Several studies have examined the behaviour of Hormuz sand, primarily using element test results [39–43]. The sand properties are presented in Table 1, and more detail can be found in Rasouli et al. [44].

Compressibility and particle shape are the primary sources of the behaviour of uncemented calcareous sand. Nauroy et al. [45] defined the tangent compressibility index (C_{pi}) as the slope of the e-log(p) curve at the pressure p_i. Le Tirant and Nauroy [46] suggested a reduction coefficient for P_u (ultimate lateral capacity of piles) as calculated using the API method, which is equal to one at $C_{pi} < 0.02$. Figure 3 shows the isotropic compression test results on Hormuz calcareous sand performed with a triaxial apparatus. The C_{pi} of dense Hormuz calcareous sand was less

Table 1 Engineering properties of Hormuz calcareous sand

C_u	C_c	D_{50} (mm)	G_s	γ_{dmin} (kN/m^3)	γ_{dmax} (kN/m^3)	e_{min}	e_{max}
1.8	0.87	0.31	2.73	14.245	17.176	0.56	0.88

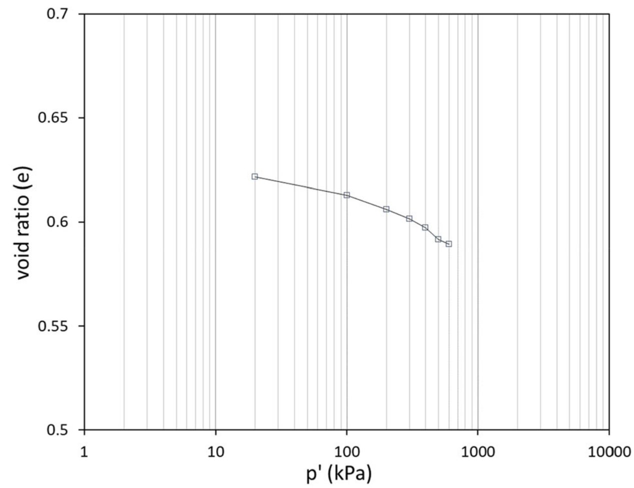

Fig. 3 Isotropic compression test results for Hormuz calcareous sand

than 0.02 for the stress range of this study. This means that it is logical to expect the overall cyclic performance of the monopile in such sand to be similar to that of a monopile in siliceous sand.

The ratio of pile diameter to median grain size was approximately 160, which is large enough to ignore the effect of grain size [47, 48]. The sand was pluviated into the container from a constant drop height. Each layer thickness was approximately 30 mm and, after every stage, the surface was levelled. The relative density was calculated by measuring the sand weight and the dimensions of the soil container.

The pile was driven into the sand at 1 g using a rubber hammer to reach the target embedment of 5*D*. Although installation at 1 g acceleration level (instead of 40 g) could significantly change the pile lateral resistance [49], its effect on the comparison between cyclic and monotonic loading, the focus of the present study, was neglected [23]. During installations, conical depressions formed around the pile. A similar phenomenon has been reported by Richards et al. [15].

2.1 Testing Program

The details of the tests are presented in Table 2. All tests were conducted at an acceleration level of 40 g and lateral loads were exerted at a height of 5.75*D* above the mudline. To determine the ultimate lateral capacity of the system and confirm the repeatability of the experiments, two monotonic tests were performed. These two tests were conducted displacement-controlled with a rate of 0.1 mm/s to ensure sufficient data collection. The sand was dry; therefore, there was no concern about the drainage situation. In monotonic tests, the purpose was to obtain the load corresponding to a displacement or rotation value;

Table 2 Test program

Test no.	Loading type	Cyclic load type	Relative density (%)	ζ_b	ζ_c	Number of cycles
M1	Monotonic	–	69	–	–	–
M2	Monotonic	–	68	–	–	–
C1	Cyclic	One way	68	0.43	− 0.03	600
C2	Cyclic	One way	69	0.65	0.01	600
C3	Cyclic	One way	69	0.28	0.01	145
C4	Cyclic	Two way	72	0.43	− 1	600
C5	Cyclic	Two way	71	0.46	− 0.53	600
C6	Cyclic	Two way	71	0.46, 0.68, 0.3	− 0.36, 0, 0.02	200, 200, 200

therefore, it was easier to measure the pile resistance to an implied displacement as is done in displacement-controlled tests.

The cyclic testing program was designed to investigate the effect of the cyclic load magnitude and symmetry on the accumulated rotation or displacement. The cyclic loading parameters were selected to cover a range of cyclic loading conditions. However, because of discrepancies in the literature regarding the effect of asymmetric two-way loading, more focus was placed on asymmetric two-way loading. In the cyclic tests, the purpose was to simulate wind and wave loading and measure the accumulated displacement and rotation. This made it more convenient to use load-controlled tests.

All the cyclic tests were designed to execute 600 cycles, but test C3 stopped after 145 cycles for unknown reasons. The cyclic loading was conducted at a frequency of 0.4 Hz, which is higher than the peak frequency of offshore waves. This frequency was chosen to apply a greater number of cycles within a certain period of time. Rate dependency is low in dry sand; therefore, it was unlikely that this change of frequency significantly affected the results [16, 23]. Test C6 was conducted to investigate the effect of loading sequence on the accumulated deformation of the monopile; however, only the first part of this test has been considered in the article.

3 Results

3.1 Monotonic Tests

The results of two monotonic tests are presented in Fig. 4. The horizontal load was normalized according to the framework suggested by LeBlanc et al. [20]. The two curves nearly overlap, which indicates the repeatability of the test procedure. Different criteria were used to determine the lateral capacity of the pile. Refs. [20, 22] defined failure at a pile rotation of 4°, while Truong et al. [27] used

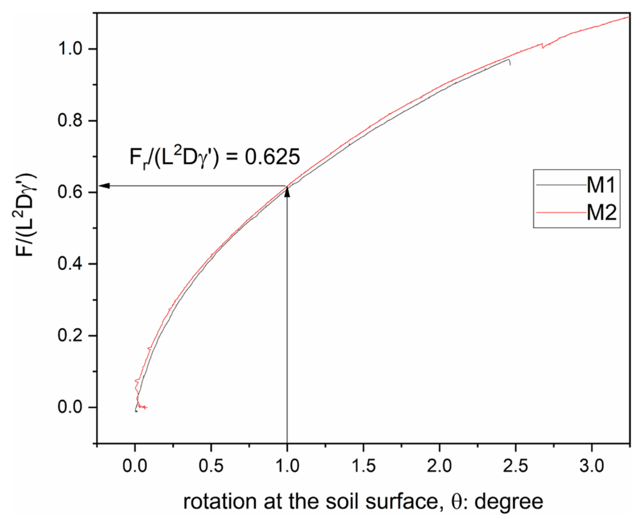

Fig. 4 Monotonic tests results showing repeatability of experiments

a ground rotation of 0.5° as the reference lateral load criterion. In the present study, a lateral load corresponding to 1° of rotation at the soil surface was chosen as the reference load. This criterion, as shown in Fig. 4, produced a normalized reference force of 0.625.

3.2 Cyclic Tests

Cyclic loading was applied in a load-controlled mode. In the first three tests (C1, C2, C3), the maximum magnitude of loading was changed, but the load reversal was kept constant. Three more tests were allocated to investigation of the effect of loading symmetry and loading reversal. The results of six cyclic tests based on rotation at the soil surface and displacement at the loading point are presented in Figs. 5 and 6, respectively. The calculated rotation at the mudline experienced more noise than did displacement at

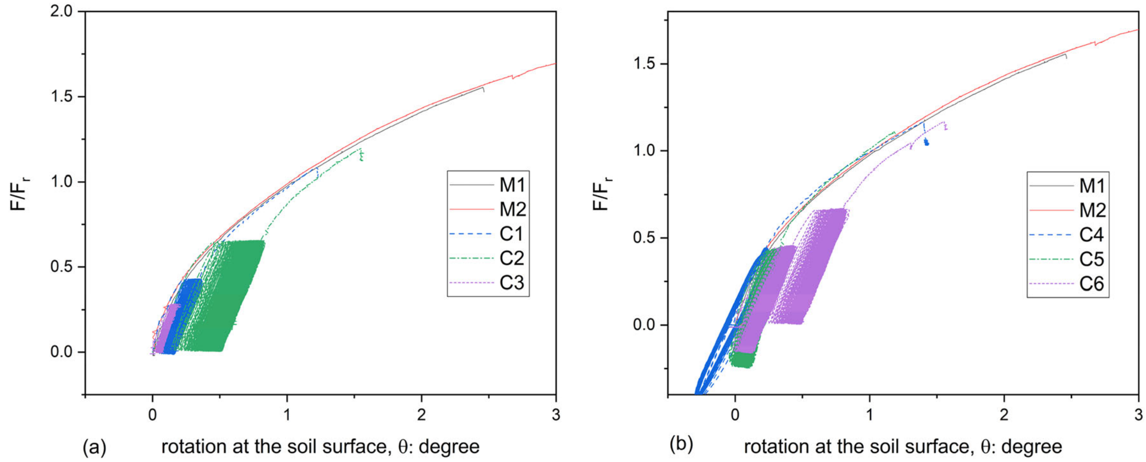

Fig. 5 Pile lateral load-rotation response: **a** $\zeta_c \approx 0$; **b** $\zeta_b \approx 0.45$

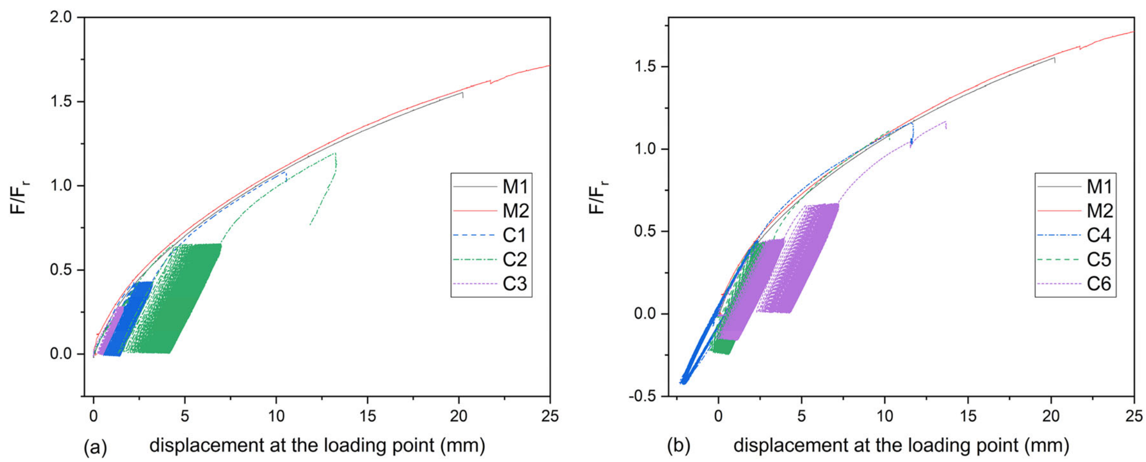

Fig. 6 Pile lateral load–displacement response: **a** $\zeta_c \approx 0$; **b** $\zeta_b \approx 0.45$

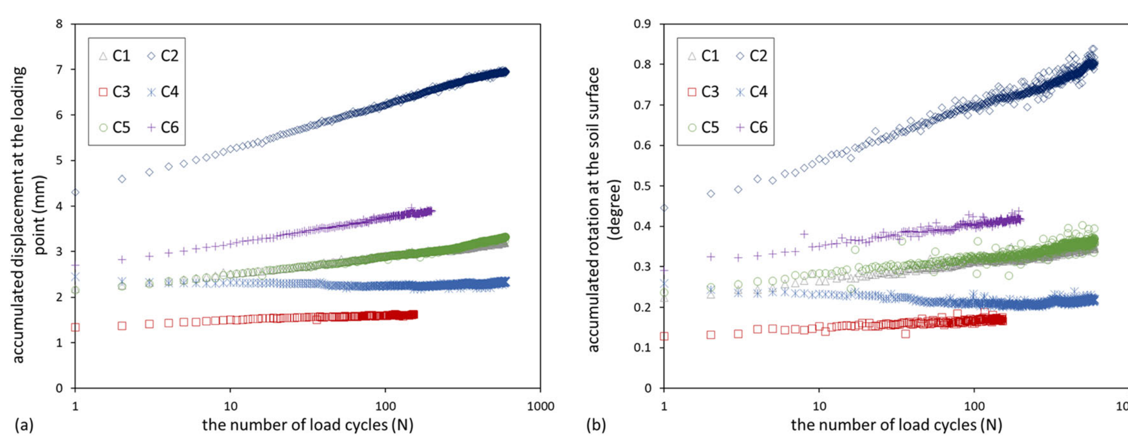

Fig. 7 **a** Maximum accumulated displacement at loading point; **b** maximum accumulated rotations at soil surface

the loading point; therefore, the latter was used in the analysis.

As stated, parameters ζ_b and ζ_c, were used to describe the cyclic loading characteristics. Parameter ζ_b is the ratio of the maximum load to F_r and denotes the magnitude of the maximum load, while ζ_c is the symmetry or reversal of cyclic loading and varies between 1 and − 1. For example,

$\zeta_c = -1$ indicates balanced two-way loading and $\zeta_c = 0$ indicates one-way loading.

Figure 7 shows the results of monopile displacement and rotation under cyclic loading. It can be seen that the change in rotation and displacement resemble each other. In all tests except for C4, in which balanced two-way loading was applied, the accumulated displacement increased as the number of cycles increased. In test C4, the accumulated displacement remained nearly constant. This indicates that the direction of the first quarter of balanced two-way loading did not determine the direction of the net accumulated displacement. Similar results for balanced two-way loading have been reported by Klinkvort and Hededal [22], but these contradict the results of Refs. [23, 24].

The slope of accumulated displacement increased with an increase in ζ_b, but the effect of ζ_c was more complex. The maximum slope occurred at $\zeta_c = -0.36$, while the slope of accumulated displacement was almost identical at ζ_c values of -0.53 and 0. Although a logarithmic function provided a better fit to the results, especially for initial cycles, the power function proposed by LeBlanc et al. [20] was used in the present study because it ensures higher accuracy at higher cycles.

Figure 8 shows the values of $\Delta y/y_1$, where y_1 is the maximum displacement during the first cycle for all cyclic tests except C5. The normalized accumulated displacement values have been fitted with the power function presented in Eq. (5). A value of $\alpha = 0.25$ was determined by averaging the fitted values of all tests, although these values were nearly identical. This value is less than the value of 0.31 reported by LeBlanc et al. [20] and greater than the values reported by Albiker et al. [26] (0.23) and Nicolai and Ibsen [10] (0.13). The fitted lines are shown in Fig. 8.

The main purpose of the deformation function was to predict the accumulated deformation at higher cycles. Therefore, the first ten cycles were excluded from fitting analysis and the focus was on higher cycles. As was expected, the accumulated displacement caused by cyclic loading (Δy) increased with an increase in the maximum magnitude:

$$\frac{\Delta y_N}{y_1} = B.N^{\alpha=0.25}, \tag{5}$$

$$B = T_b(\zeta_b.R_d)T_c(\zeta_c). \tag{6}$$

In these equations, T_c takes into account the effect of loading symmetry or reversal. When one-way loading ($\zeta_c = 0$) was applied, the output of T_c was assumed to be equal to 1; therefore, by calculating the fitting curve coefficient (B) for tests in which one-way loading was applied (C1, C2, C3), the value of T_b could be calculated. Figure 9 shows the values of T_b based on ζ_b, where ζ_c is approximately zero. The fitted line was forced to have a zero intercept because it is not possible to have accumulated displacement without a cyclic load. The results were also compared with those of other studies [10, 20]. It should be noted that LeBlanc et al. [20] defined pile lateral capacity at a pile rotation of 4° while Nicolai and Ibsen [10] used ultimate resistance. In the present study, the 1° criterion was used; therefore, the ζ_b values in Fig. 9 are not directly comparable. The relationship between T_b and ζ_b in the present research can be described as:

$$T_b = 0.212\zeta_b. \tag{7}$$

The effect of loading reversal on accumulated displacement was investigated by changing ζ_c while holding ζ_b constant. The value of T_c was calculated by dividing the fitting curve coefficient extracted from Fig. 8 [B in Eq. (6)]

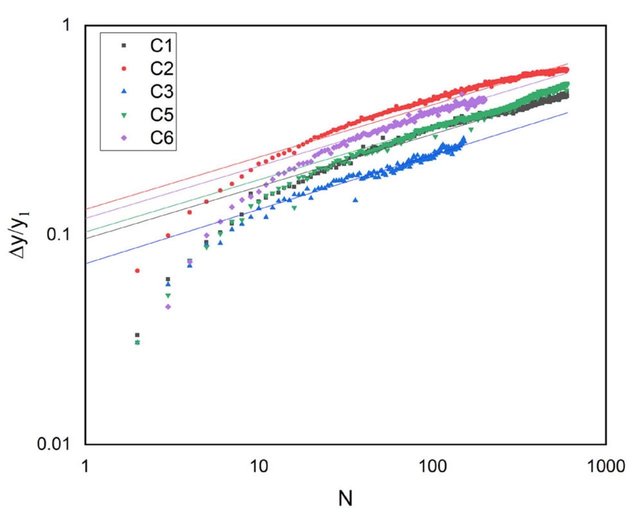

Fig. 8 Normalized pile displacements at loading point. Lines obtained using Eq. (5)

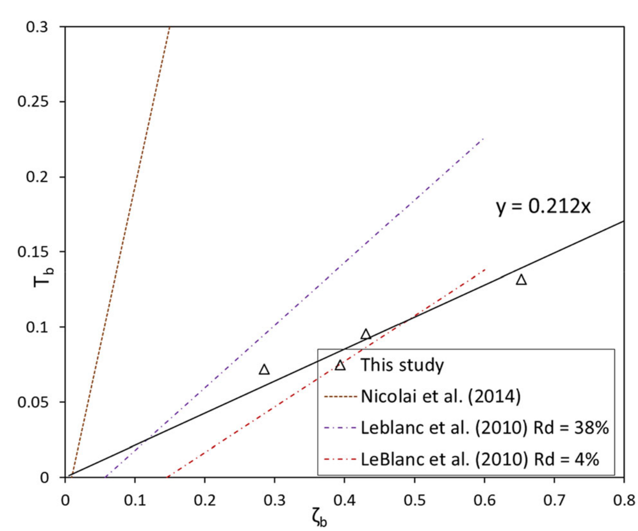

Fig. 9 T_b function in terms of ζ_b

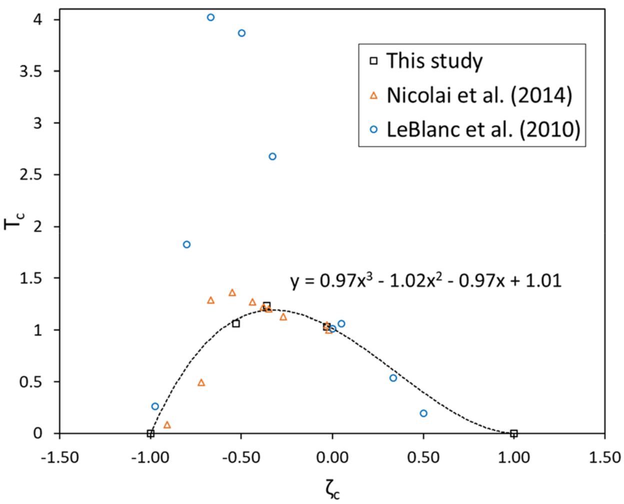

Fig. 10 T_c function in terms of ζ_c

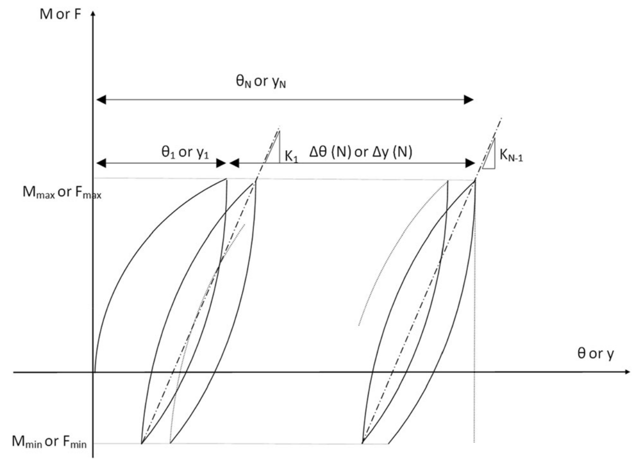

Fig. 11 Definition of cyclic parameters [27]

by the T_b value estimated from Eq. (7). The results are presented in Fig. 10. By definition, the value of T_c in the case of static loading ($\zeta_c = 0$) should be equal to zero. In test C4, when loading approached the balanced two-way condition, the accumulated displacement remained constant; therefore, the value of T_c for $\zeta_c = -1$ was considered to be zero. It can be seen that a third-order polynomial fits the data in Eq. (8):

$$T_c = 0.97\zeta_c^3 - 1.02\zeta_c^2 - 0.97\zeta_c + 1.01. \quad (8)$$

The shape of the derived T_c function is similar to the one reported by Refs. [10, 20, 26]; however, the maximum value was much less than the one described by LeBlanc et al. [20]. The results show that partially unbalanced loading ($\zeta_c = -0.35$) was the most damaging condition. This is in line with the observations of Refs. [20, 26, 50], but contradict the results of Klinkvort and Hededal [22].

The foundation stiffness is an essential aspect of the design of OWT foundations. There are discrepancies in the definitions of secant stiffness in the literature. In the present study, secant stiffness has been defined as the ratio of the difference between the peak values of the lateral load in a cycle to the difference between the corresponding displacements (see Fig. 11). Other studies [16, 51] have used a similar definition.

In Fig. 12, the calculated secant stiffness (prototype scale) is presented against the number of cycles in the logarithmic scale. As can be seen, stiffness always increased with an increase in the number of cycles; however, the amount of increase was less than that reported by some researchers. For example, the maximum increase in stiffness was observed in test C2, but this was only about 15%, which is much less than the amount reported by Refs. [22, 27]. Part of this dissimilarity could be from the use of different definitions.

As shown in Fig. 12, the change in stiffness could be described by a logarithmic law. The slope of the line was governed by the magnitude of cyclic loading (ζ_b) and increased with an increase in ζ_b. On the other hand, the load reversal condition only slightly affected the slope. These results show that the Y-interval (K_1) was dependent on both loading parameters. K_1 decreased with an increase in the cyclic loading magnitude as a result of the nonlinear behaviour of the soil-pile system, as shown in Fig. 12a. For ζ_c, K_1 was nearly constant when ζ_c varied from 0 to -0.55 and then dropped rapidly at $\zeta_c = -1$, indicating balanced two-way loading. The change in stiffness can be expressed as:

$$K_N = K_1 + A_k(\zeta_b).\ln(N), \quad (9)$$

$$K_1 = k_b(\zeta_b).k_c(\zeta_c), \quad (10)$$

where K_1 and K_N are the stiffness in the first cycle and in cycle number N, respectively (Fig. 11), and A_k is a dimensionless coefficient. LeBlanc et al. [20] assumed A_k to be constant, but the results of the present study show that it is a function of ζ_b.

Figure 5 shows that, in all tests except C3, monotonic loading was applied after cyclic loading. Figure 13 presents the post-cyclic response. Similar trends were observed for the rotation-based response. The post-cyclic response of the monopiles in all tests except for C2 and C6 was nearly the same as for the virgin monotonic response at high loading magnitudes. In tests C2 and C6, the post-cyclic capacity did not reach the static capacity. In these two tests, the monopile was subjected to higher loading magnitudes; therefore, cyclic loading caused more permanent displacement than in the other tests.

There could be a threshold in the permanent displacement or the cyclic load magnitude beyond which post-cycle resistance decreases. Truong et al. [27] observed a similar phenomenon. In their tests with a permanent rotation of

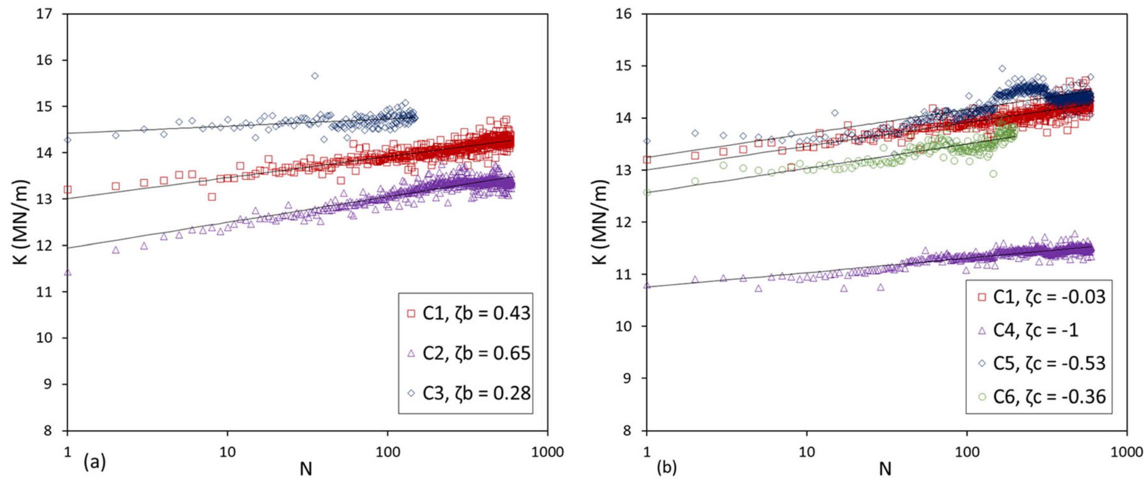

Fig. 12 Calculated secant stiffness: **a** $\zeta_c \approx 0$; **b** $\zeta_b \approx 0.45$

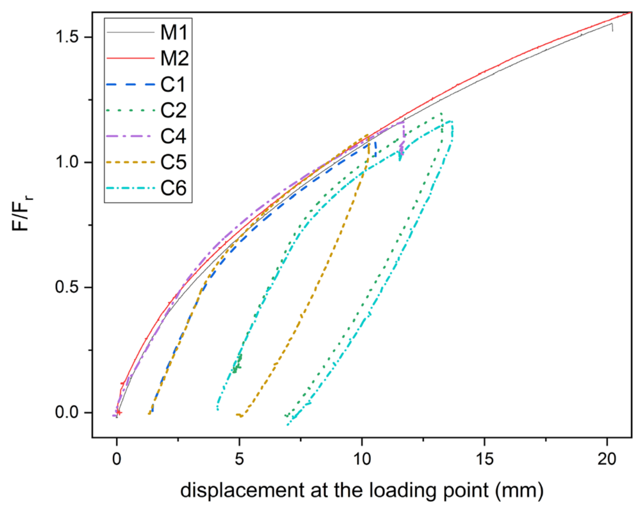

Fig. 13 Post-cyclic response

greater than 0.5°, post-cyclic resistance was lower than for monotonic resistance. On the other hand, Nicolai et al. [14] stated that the monotonic resistance increased after cyclic loading. Although the permanent rotation of the monopile in tests C2 and C6 was greater than 0.5°, more data are needed to reach a firm conclusion on this. The decrease in resistance could be due to experimental error.

Figure 14 shows the bending moment diagrams measured by ten pairs of strain gauges along the pile length. The results show that the maximum bending moment increased slightly after 600 cycles; however, the depth of the maximum moment remained almost constant. It should be noted that part of this increase was due to small differences in the lateral load magnitude. In most tests, the maximum bending moment at the point of zero lateral loads increased significantly.

Kirkwood and Haigh [12] used the term "locked-in moments" to describe non-zero bending moments in piles when no loading was applied. As shown in Fig. 14, the maximum locked-in moment occurred around the middle of the pile embedment length. The change in the locked-in moment magnitude with the number of cycles is shown in Fig. 15. The slope of increase in the locked-in moments appears to be dependent on ζ_c. In tests C1 and C2, where ζ_c was approximately zero, the increases in the locked-in moments had similar slopes. In test C5, where balanced two-way loading was applied, the locked-in moments were almost constant. In the tests where $\zeta_c < 0$, there were two moments in every cycle when the applied force was equal to zero. The locked-in moments for both of these moments are presented in Fig. 14. The results showed that, after a negative peak, the locked-in moment was negative and, after a positive peak, it was positive. However, in both cases, the magnitude of the locked-in moments was less than for the one-way loading test at equal values of ζ_b.

The existence of a locked-in moment indicates a change of density and stress caused by cyclic loading. Kirkwood and Haigh [12] attributed the greater pile displacement in the case of unbalanced two-way loading to the fact that, in that case, the locked-in moment was smaller than when one-way loading was applied. However, in the current study, the lower residual moment in balanced two-way loading did not increase displacement.

4 Conclusions

A series of centrifuge model tests were performed to investigate the effects of the loading characteristics on monopiles in dense calcareous sand. Parameters ζ_b and ζ_c were used to describe the cyclic loading magnitude and reversal, respectively. The following conclusions have been drawn:

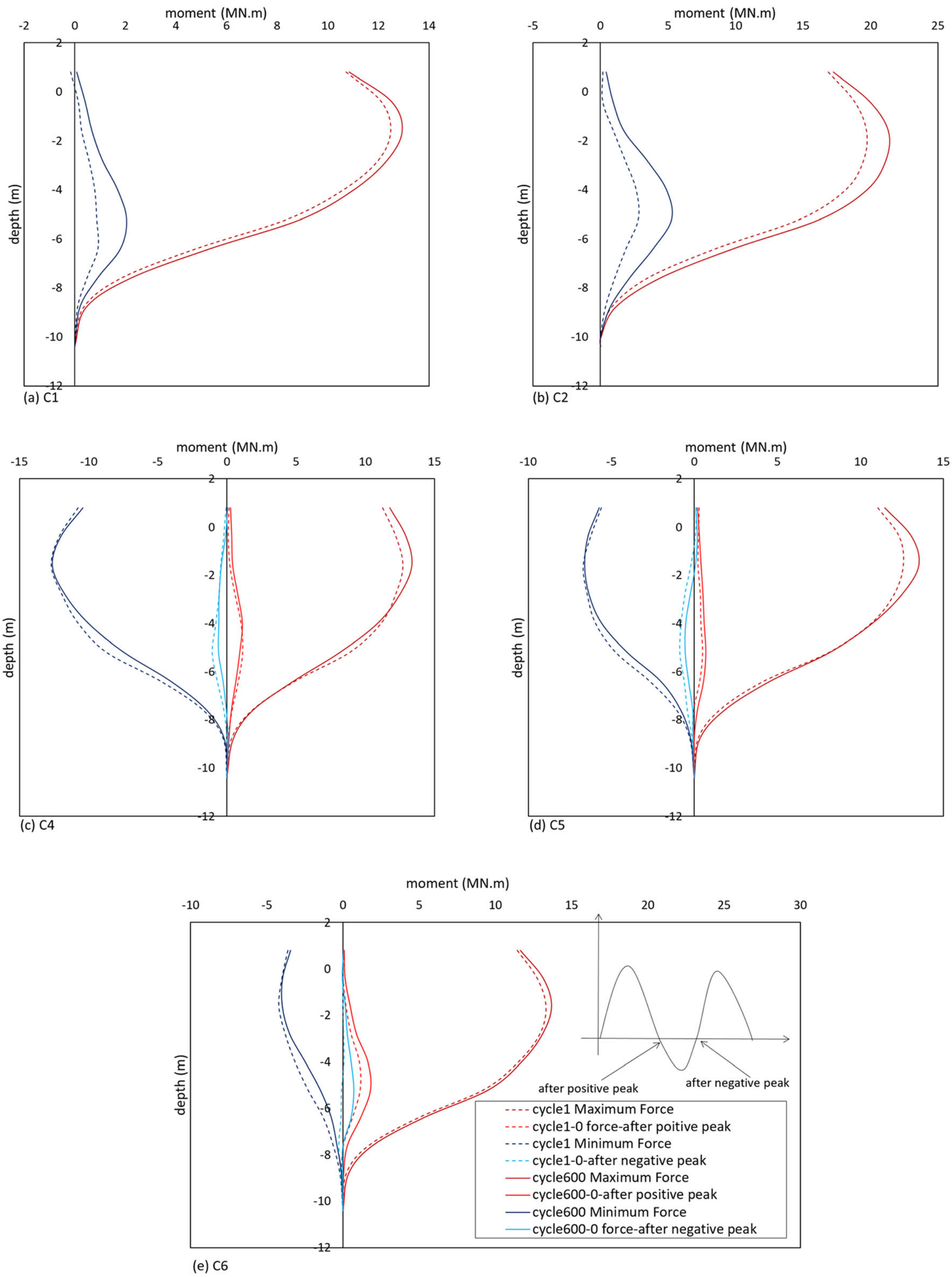

Fig. 14 Bending moment profiles along monopile in cyclic tests

- The accumulated displacement increased as a power function of the number of cycles. This function was strongly affected by the loading characteristics. Partially unbalanced loading was the most damaging loading condition. The model proposed by LeBlanc et al. [20] was adopted to predict the accumulated displacement.

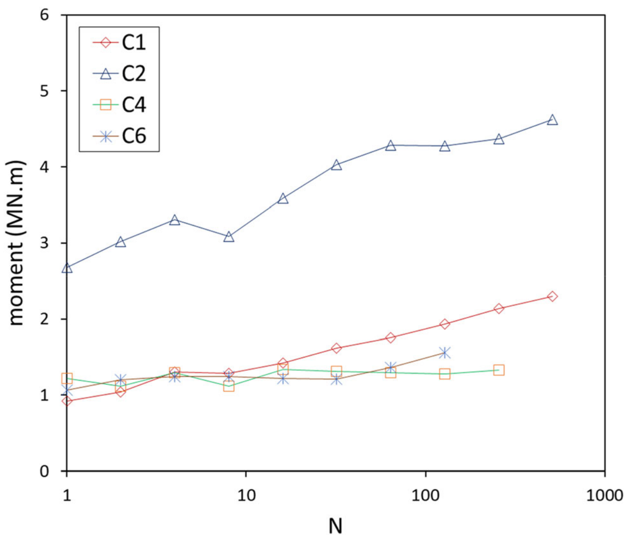

Fig. 15 Bending moment in monopile at 5.2 m in depth at zero lateral load

- For balanced two-way loading (symmetric loading), the accumulated displacement almost remained constant; however, the soil-pile stiffness increased.
- The secant stiffness of the soil-pile system increased moderately as cyclic loading proceeded. A logarithmic function has been used to express the variation in stiffness. The slope of this function increased with an increase in the maximum load magnitude (ζ_b), although stiffness was lower for tests with higher ζ_b values. Nevertheless, ζ_c did not affect the slope of this function. Furthermore, in the test with balanced two-way loading ($\zeta_c = -1$), the secant stiffness was considerably lower than for the other tests.
- After cyclic loading, monotonic loading was applied. In most tests, except for tests with a higher magnitude of cyclic loading, the post-cyclic capacity was almost equal to the static capacity. This indicates that there could have been a threshold for the maximum cyclic load magnitude or permanent displacement beyond which the post-cyclic resistance decreased.
- The magnitude of locked-in moments in tests with one-way loading increased but remained relatively constant in the balanced two-way loading test. The maximum locked-in moments occurred at the middle of the pile in all tests.

The overall behaviour of the monopile in calcareous sand was similar to that previously reported for siliceous sand, and it appears that crushability did not affect the monopile behaviour, probably because of the low level of stress.

Acknowledgements Not applicable.

Declarations

Conflict of interest On behalf of all authors, the corresponding author states that there is no conflict of interest.

References

1. Rasmussen KL, Hansen M, Kirk Wolf T, Ibsen L B, Roesen HR (2013) A literature study on the effects of cyclic lateral loading of monopiles in cohesionless soils. In: DCE technical memorandum, no. 025, Department of Civil Engineering, Aalborg University, Aalborg
2. American Petroleum Institute (2014) Recommended practice 2GEO—geotechnical and foundation design considerations. API, Washington
3. DNV (Det Norske Veritas) (2011) DNV-OS-J101: design of offshore wind turbine structures. DNV, Oslo
4. Reese LC, Cox WR, Koop FD (1974) Analysis of laterally loaded piles in sand. In: Offshore technology conference, Houston, pp 473–483. https://doi.org/10.4043/2080-MS
5. O'Neill MW, Murchison JM (1983) An evaluation of py relationships in sands. In: A report to the American Petroleum Institute. Report no. GTDF02-83. Department of Civil Engineering, University of Houston
6. Lesny K, Wiemann J (2006) Finite-element-modelling of large diameter monopiles for offshore wind energy converters. In: GeoCongress 2006. American Society of Civil Engineers, Reston, VA, pp 1–6. https://doi.org/10.1061/40803(187)212
7. Achmus M, Abdel-Rahman K, Kuo Y-S (2008) Design of monopile foundations for offshore wind energy converters. In: Proceeding of 11th baltic sea geotechnical conference, goetechnics in maritime engineering. Gdansk, pp 463–470
8. Li W, Zhu B, Yang M (2017) Static response of monopile to lateral load in overconsolidated dense sand. J Geotech Geoenviron Eng. https://doi.org/10.1061/(ASCE)GT.1943-5606.0001698
9. Alamouti SD, Moradi M, Bahaari MR (2018) Centrifuge modelling of monopiles subjected to lateral loading. Scientia Iranica 26(6):3109–3124. https://doi.org/10.24200/sci.2018.20222
10. Nicolai G, Ibsen LB (2014) Small-scale testing of cyclic laterally loaded monopiles in dense saturated sand. J Ocean Wind Energy 1(4):240–245
11. Zhang X, Zhang C, Liu Y, Hu Z (2020) Nondimensional parametric method for studying lateral cyclic response of offshore monopiles in sand. Mar Georesour Geotechnol. https://doi.org/10.1080/1064119X.2020.1717696
12. Kirkwood PB, Haigh SK (2014) Centrifuge testing of monopiles subject to cyclic lateral loading. In: Proceedings of the 8th international conference on physical modelling in Geotechnics, pp 827–831
13. Achmus M, Kuo YS, Abdel-Rahman K (2009) Behavior of monopile foundations under cyclic lateral load. Comput Geotech 36(5):725–735. https://doi.org/10.1016/j.compgeo.2008.12.003
14. Nicolai G, Ibsen LB, O'Loughlin CD, White DJ (2017) Quantifying the increase in lateral capacity of monopiles in sand due to cyclic loading. Géotech Lett 7(3):245–252. https://doi.org/10.1680/jgele.16.00187
15. Richards IA, Byrne BW, Houlsby GT (2020) Monopile rotation under complex cyclic lateral loading in sand. Géotechnique 70(10):916–930. https://doi.org/10.1680/jgeot.18.P.302
16. Abadie CN, Byrne BW, Houlsby GT (2019) Rigid pile response to cyclic lateral loading: laboratory tests. Géotechnique 69(10):863–876. https://doi.org/10.1680/jgeot.16.P.325

17. Little RL, Briaud J-L (1988) Full scale cyclic lateral load tests on six single piles in sand. In: Miscellaneous paper GL-88-27. Geotechnical division, Texas A&M University, Texas
18. Long JH, Vanneste G (1994) Effects of cyclic lateral loads on piles in sand. J Geotech Eng 120(1):225–244. https://doi.org/10.1061/(ASCE)0733-9410(1994)120:1(225)
19. Lin S-S, Liao J-C (1999) Permanent strains of piles in sand due to cyclic lateral loads. J Geotech Geoenviron Eng 125(9):798–802. https://doi.org/10.1061/(ASCE)1090-0241(1999)125:9(798)
20. LeBlanc C, Houlsby GT, Byrne BW (2010) Response of stiff piles in sand to long-term cyclic lateral loading. Géotechnique 60(2):79–90. https://doi.org/10.1680/geot.7.00196
21. Kirkwood PB, Haigh SK (2013) Centrifuge testing of monopiles for offshore wind turbines. In: Proceedings of the twenty-third international offshore and polar engineering conference, ISOPE, Anchorage, AK, pp 126–130
22. Klinkvort RT, Hededal O (2013) Lateral response of monopile supporting an offshore wind turbine. Proc Inst Civ Eng Geotech Eng 166(2):147–158. https://doi.org/10.1680/geng.12.00033
23. Rosquoet F, Thorel L, Garnier J, Canepa Y (2007) Lateral cyclic loading of sand-installed piles. Soils Found 47(5):821–832. https://doi.org/10.3208/sandf.47.821
24. Arshad M, O'Kelly BC (2017) Model studies on monopile behavior under long-term repeated lateral loading. Int J Geomech 17(1):04016040. https://doi.org/10.1061/(ASCE)GM.1943-5622.0000679
25. Cuéllar VP (2011) Pile foundations for offshore wind turbines: numerical and experimental investigations on the behaviour under short-term and long-term cyclic loading. PhD thesis, Technical University of Berlin
26. Albiker J, Achmus M, Frick D, Flindt F (2017) 1 g model tests on the displacement accumulation of large-diameter piles under cyclic lateral loading. Geotech Test J 40(2):173–184. https://doi.org/10.1520/GTJ20160102
27. Truong P, Lehane BM, Zania V, Klinkvort RT (2019) Laterally loaded piles in sand empirical approach based on centrifuge testing for cyclic deformations of laterally loaded piles in sand. Géotechnique 69(2):133–145. https://doi.org/10.1680/jgeot.17.P.203
28. Holmes A (1965) Principles of physical geology, 2nd edn. Thomas Nelson, London
29. Murff JD (1987) Pile capacity in calcareous sands: state if the art. J Geotech Eng 113(5):490–507. https://doi.org/10.1061/(ASCE)0733-9410(1987)113:5(490)
30. Dyson GJ, Randolph MF (2001) Monotonic lateral loading of piles in calcareous sand. J Geotech Geoenviron Eng 127(4):346–352. https://doi.org/10.1061/(ASCE)1090-0241(2001)127:4(346)
31. Wesselink BD, Murff JD, Randolph MF, Nunez IL, Hyden AM (1988) Analysis of centrifuge model test data from laterally loaded piles in calcareous sand. Eng Calcareous Sedim 1:261–270
32. Moradi M, Rojhani M, Galandarzadeh A, Takada S (2013) Centrifuge modeling of buried continuous pipelines subjected to normal faulting. Earthq Eng Eng Vib 12(1):155–164. https://doi.org/10.1007/s11803-013-0159-z
33. Choo YW, Kim D (2016) Experimental development of the p-y relationship for large-diameter offshore monopiles in sands: centrifuge tests. J Geotech Geoenviron Eng 142(1):04015058. https://doi.org/10.1061/(ASCE)GT.1943-5606.0001373
34. Poulos HG, Hull T (1989) The role of analytical geomechanics in foundation engineering. Found Eng Curr Princ Pract 2:1578–1606
35. Abadie CN (2015) Cyclic lateral loading of monopile foundations in cohesionless soils. University of Oxford
36. Achmus M, Abdel-Rahman K, Kuo YS (2007) Numerical modelling of large diameter steel piles under monotonic and cyclic horizontal loading. In: Proceedings of the 10th international symposium on numerical models in geomechanics, Rhodes, pp 453–459
37. Madabhushi GS, Haiderali AE (2013) Evaluation of the py method in the design of monopiles for offshore wind turbines. In: Offshore technology conference, Houston, pp 1824–1844
38. Bhattacharya S, Nikitas N, Garnsey J, Alexander NA, Cox J, Lombardi D, Wood DM, Nash DF (2013) Observed dynamic soil–structure interaction in scale testing of offshore wind turbine foundations. Soil Dyn Earthq Eng 54:47–60. https://doi.org/10.1016/j.soildyn.2013.07.012
39. Hassanlourad M, Salehzadeh H, Shahnazari H (2010) Mechanical properties of ungrouted and grouted carbonate sands. Int J Geotech Eng 4(4):507–516. https://doi.org/10.3328/IJGE.2010.04.04.507-516
40. Goodarzi S, Shahnazari H (2019) Strength enhancement of geotextile-reinforced carbonate sand. Geotext Geomembr 47(2):128–139. https://doi.org/10.1016/j.geotexmem.2018.12.004
41. Shahnazari H, Maghoul M, Alizadeh M, Saeedi Javadi A (2018) Effect of anisotropy on shear behavior of Hormoz carbonate sand. Int J Geotech Eng 12(5):484–490. https://doi.org/10.1080/19386362.2017.1297759
42. Hassanlourad M, Rasouli MR, Salehzadeh H (2014) A comparison between the undrained shear behavior of carbonate and quartz sands. Int J Civ Eng 12(4):338–350
43. Jafarian Y, Javdanian H, Haddad A (2018) Dynamic properties of calcareous and siliceous sands under isotropic and anisotropic stress conditions. Soils Found 58:172–184. https://doi.org/10.1016/j.sandf.2017.11.010
44. Rasouli MR, Moradi M, Ghalandarzadeh A (2020) Effects of initial static shear stress orientation on cyclic behavior of calcareous sand. Mar Georesour Geotechnol 18:1–5. https://doi.org/10.1080/1064119X.2020.1726535
45. Nauroy JF, Brucy F, Le Tirant P, Kervadec JP (1986) Design and installation of piles in calcareous formations. In: Proceedings of 3rd international conference of numerical methods in offshore piling, Nantes pp 461–480
46. Le Tirant P, Nauroy J-F (eds) (1994) Design guides for offshore structures: foundations in carbonate soils. Editions Technip, Paris
47. Remaud D (1999) Physical modeling of pile under lateral loads: interpretation problem and of validation, Comptes-rendus du prix jeune chercheur 99, 2 cong. University de Genie Civil AUGC, Poitiers, pp 185–192
48. Garnier J, Gaudin C, Springman SM, Culligan PJ, Goodings D, Konig D, Kutter B, Phillips R, Randolph MF, Thorel L (2007) Catalogue of scaling laws and similitude questions in geotechnical centrifuge modelling. Int J Phys Modell Geotech 7(3):01–23. https://doi.org/10.1680/ijpmg.2007.070301
49. Fan S, Bienen B, Randolph MF (2021) Centrifuge study on effect of installation method on lateral response of monopiles in sand. Int J Phys Modell Geotech 21(1):40–52. https://doi.org/10.1680/jphmg.19.00013
50. Roesen HR, Ibsen LB, Andersen LV (2013) Experimental testing of monopiles in sand subjected to one-way long-term cyclic lateral loading. In: Proceedings of the 18th international conference on soil mechanics and geotechnical engineering, Paris, pp 2391–2394
51. Li Q, Askarinejad A, Gavin K (2020) Lateral response of rigid monopiles subjected to cyclic loading: centrifuge modelling. Proc Inst Civ Eng Geotech Eng 11:1–3. https://doi.org/10.1680/jgeen.20.00088